Estimating the Resolution of Nanopositioning Systems from Frequency Domain Data

Andrew J. Fleming[†]
School of Electrical Eng. and Computer Science
The University of Newcastle
NSW 2300, Australia
andrew.fleming@newcastle.edu.au

Abstract— Mechanical and electrical noise in nanopositioning systems is unavoidable and dictates the maximum positioning resolution. The proper specification of resolution is critical for defining the smallest possible dimensions in a manufacturing processes or the smallest measurable features in an imaging application. This article defines a standard for the reporting of resolution and demonstrates how this parameter can be measured and predicted from frequency domain data.

I. INTRODUCTION

A nanopositioning system is an electromechanical device for maneuvering an object in three or more degrees of freedom. A typical nanopositioner consists of base, a moving platform, actuators, position sensors, and a control system [1]. These devices are commonly used in scanning probe microscopes [2] to develop displacements of between one and one-hundred micrometers with a resolution on the order of one nanometer or less. Other applications of nanopositioning systems include nanofabrication [3], data storage [4], cell surgery, beam pointing, and precision optical alignment.

A key performance specification of a nanopositioner, or indeed many other controlled systems, is the resolution. The resolution is essentially the amount of random variation that remains at the output, even when the system is at rest. The resolution is critical for defining the smallest possible dimensions in a manufacturing processes or the smallest measurable features in an imaging application.

Although the resolution is a key performance criteria in many applications, there is unfortunately no strict definition available in the literature. There are also no published industrial standards for the measurement or reporting of positioning resolution. Predictably, this has led to a wide variety of fragmented techniques used throughout both academia and industry. As a result, it is extremely difficult to compare the performance of different control strategies or commercial products.

The most reliable method for the measurement of resolution is to utilize an auxiliary sensor that is not involved in the feedback loop. However, this requires a sensor with less additive noise and greater bandwidth than the displacement to be measured. Due to these strict requirements, the direct measurement approach is often impractical or impossible. Instead, the closed-loop positioning noise is usually predicted from measurements of known noise sources such as the sensor noise.

In industrial and commercial applications, the methods used to measure and report closed-loop resolution are widely varied. Unfortunately, many of these techniques do not provide complete information and may even be misleading. For example, the RMS noise and resolution is commonly reported without mention of the closed-loop or measurement bandwidth. In the academic literature, the practices for reporting noise and resolution also vary. The most common approach is to predict the closed-loop noise from measurements of the sensor noise [4], [5]. However, this approach can underestimate the true noise since the influence of the high-voltage amplifier is neglected. In the hard drive industry, the standard performance metric for resolution is the track pitch and the standard deviation of the measurement [6], [7]. However, the main sources of error in a disk drive are due to aeroelastic effects and track eccentricities which are not present in a nanopositioning system.

In this article, the resolution is defined as the minimum distance between two points that can be uniquely identified. Although the focus is on nanopositioning applications, the background theory and measurement techniques are applicable to any control system where resolution is a factor.

II. RESOLUTION AND NOISE

When a nanopositioner has settled to a commanded location, a small amount of random motion remains due to sensor noise, amplifier noise, and external disturbances. The residual random motion means that two adjacent commanded locations may actually overlap, which can cause manufacturing faults or imaging artefacts. To avoid these eventualities, it is critical to know the minimum distance between two adjacent points that can be uniquely identified.

Since the noise sources that contribute to random position errors can have a potentially large dispersion, it is impractically conservative to specify a resolution where adjacent points never overlap. Instead, it is preferable to state the probability that the actual position is within a certain error bound. Consider the example of random positioning errors plotted in Figure 1(a). Observe that the peak-to-peak amplitude of random motion is bounded by δ_x and δ_y, however this range is occasionally exceeded. If the random position variation is assumed to be Gaussian distributed, the probability density functions of three adjacent points, spaced by δ_x, are plotted in Figure 1(b). In this example, δ_x is equal to $\pm 3\sigma_x$ or $6\sigma_x$ which means that 99.7% of the samples fall within the range specified by δ_x. Restated, there is a 0.3% chance that the position is exceeding δ_x and straying into a neighboring area, this probability is shaded in grey.

For many applications, a 99.7% probability that the position falls within $\delta_x = 6\sigma_x$ is an appropriate definition for the resolution. To be precise, this definition should be referred to as the 6σ-resolution and specifies the minimum spacing between two adjacent points that do not overlap 99.7% of the time. Although there is no international standard for the measurement or reporting of resolution in a positioning system,
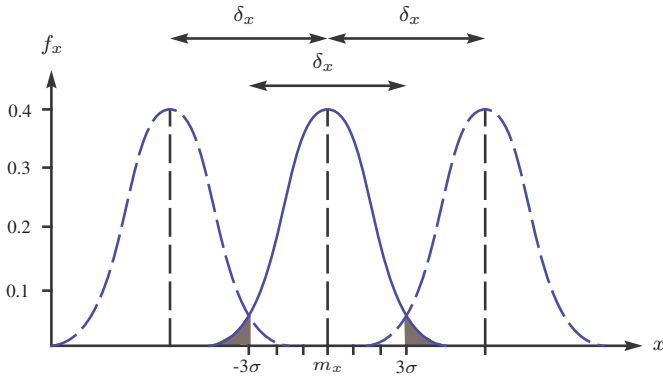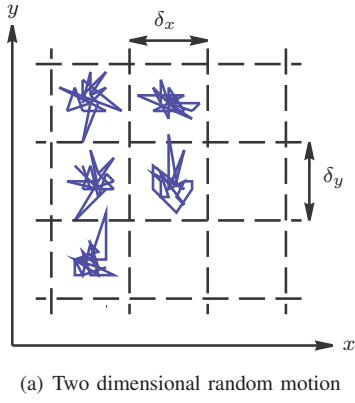
(a) Two dimensional random motion

(b) The probability density functions of three adjacent points on the x-axis

Fig. 1. The random motion of a two-dimensional nanopositioner. The random motion in the x and y-axis is bounded by δ_x and δ_y. In the x-axis, the standard deviation and mean are σ_x and m_x respectively. The shaded areas represent the probability of the position being outside the range specified by δ_x.

the ISO 5725 Standard on Accuracy (Trueness and Precision) of Measurement Methods and Results [8] defines precision as the standard deviation (RMS Value) of a measurement. Thus, the 6σ-resolution is equivalent to six times the ISO definition for precision.

III. SOURCES OF NANOPOSITIONING NOISE

The three major sources of noise in a nanopositioning systems are the sensor noise, external noise, and the amplifier output voltage noise. The power spectral density of each source is derived in the following to allow the estimation of closed-loop position noise.

A. Sensor noise

The noise characteristics of a position sensor depend mainly on the physical method used for detection. Although there are a vast range of sensing techniques available, for the purpose of noise analysis, these can be grouped into two categories: baseband sensors, and modulated sensors.

Baseband sensors involve a direct measurement of position from a physical variable that is sensitive to displacement. Examples include resistive strain sensors, piezoelectric strain sensors and optical triangulation sensors [9], [10]. The power spectral density of a baseband sensor is typically described by the sum of white noise and $1/f$ noise, where $1/f$ noise has a power spectral density that is inversely proportional to frequency [11], [12]. $1/f$ noise is used to
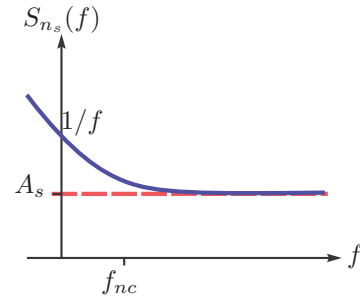

Fig. 2. Power spectral density of a baseband sensor (solid line) and a modulated sensor (dashed line). A_s is the noise density and f_{nc} is the $1/f$ noise corner frequency.

approximate the power spectrum of physical processes such as flicker noise in resistors and current noise in transistor junctions. The power spectral density of a baseband sensor $S_{n_s}(f)$ can be written

$$S_{n_s}(f) = A_s \frac{f_{\text{nc}}}{|f|} + A_s, \tag{1}$$

where A_s is the mid-band density, expressed in units^2/Hz and f_{nc} is the $1/f$ corner frequency. This function is plotted in Figure 2.

In contrast to baseband sensors, modulated sensors use a high-frequency excitation to detect position. Examples include capacitive sensors, eddy-current sensors, and Linear Variable Displacement Transformers (LVDTs) [9]. Although these sensors require a demodulation process that inevitably adds noise, this disadvantage is usually outweighed by the removal of $1/f$ noise. The power spectral density $S_{n_s}(f)$ of a modulated sensor can generally be approximated by

$$S_{n_s}(f) = A_s, \tag{2}$$

where A_s is the noise density, expressed in units^2/Hz. The power spectral density of a modulated sensor is compared to a baseband sensor in Figure 2.

In nanopositioning applications, modulated sensors can be preferable to baseband sensors as they do not exhibit $1/f$ noise. Thus, in the following, the focus is on modulated sensors with an approximately constant noise spectral density.

B. External noise

The external force noise exerted on a nanopositioner is highly dependent on the ambient environmental conditions and can not be generalized. Typically, the power spectral density consists of broad spectrum background vibration with a number of narrow band spikes at harmonic frequencies of the mains power source and any local rotating machinery. Although the external force noise must be measured in-situ, for the purposes of simulation, it is useful to assume a white power spectral density A_w, that is

$$S_w(f) = A_w. \tag{3}$$

Clearly a white power spectral density does not provide an accurate estimate of externally induced position noise. However, it does illustrate the response of the control system to noise from this source. That is, it reveals whether the control system attenuates or amplifies external noise and over what frequency regions. A constant power spectral density of A_w is used for this purpose in the following sections.
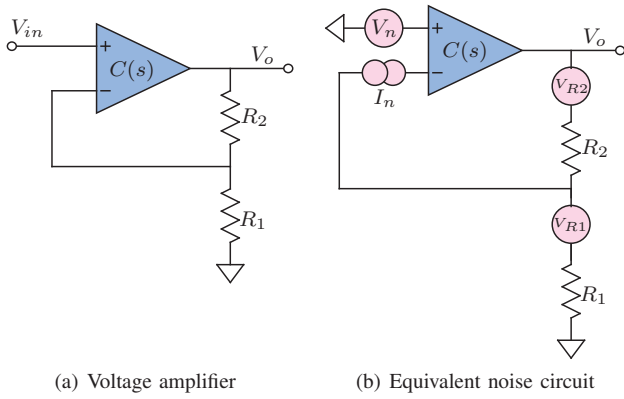
(a) Voltage amplifier   (b) Equivalent noise circuit

Fig. 3. The simplified schematic of a voltage amplifier and its equivalent noise circuit. The noise sources V_n and I_n represent the equivalent input voltage noise and current noise of the amplifier. V_{R1} and V_{R2} are the thermal noise of the feedback resistors.
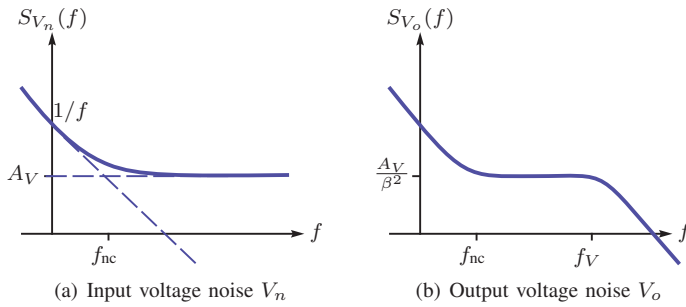

(a) Input voltage noise V_n (b) Output voltage noise V_o

Fig. 4. Power spectral density of the input and output voltage noise of a high-voltage amplifier. f_{nc} is the noise corner frequency.

C. Amplifier noise

The high-voltage amplifier is a key component of any piezoelectric actuated system. It amplifies the control signal from a few volts up to the hundreds of volts required to obtain full stroke from the actuator. For the purpose of noise analysis, the simplified schematic diagram of a non-inverting amplifier in shown in Figure 3(a). This model is sufficient to represent the characteristics of interest. The opamp represents the differential gain stage and output stage of the amplifier. As high-voltage amplifiers are often stabilized by a dominant pole, the open-loop dynamics can be approximated by a high-gain integrator $C(s) = \alpha_{ol}/s$, where α_{ol} is the open-loop DC gain. With this approximation, the closed-loop transfer function is

$$\frac{V_o}{V_{in}} = \frac{1}{\beta} \frac{\alpha_{ol}\beta}{s + \alpha_{ol}\beta}, \tag{4}$$

where β is the feedback gain $\frac{R_1}{R_2+R_1}$. The closed-loop DC gain and bandwidth are:

$$\text{DC Gain} = \frac{1}{\beta} = \frac{R_2 + R_1}{R_1}, \tag{5}$$

$$\text{Bandwidth} = \alpha_{ol}\beta = \alpha_{ol}\frac{R_1}{R_2 + R_1} \quad \text{rad/s.}$$

The input voltage noise of a practical high-voltage amplifier can be approximated by the sum of a white noise
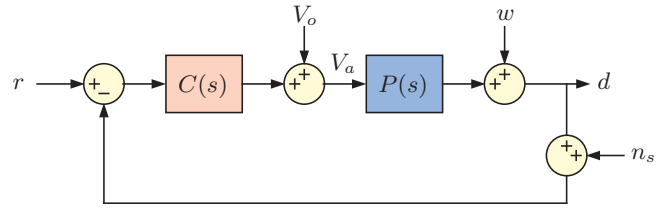
process and $1/f$ noise, that is, the power spectral density can be written

$$S_{V_n}(f) = A_V \frac{f_{nc}}{|f|} + A_V. \tag{6}$$

where f_{nc} is the noise corner frequency and A_V is the mid-band density, expressed in V^2/Hz. The power spectral density of the amplifier output voltage is then approximately

$$S_{V_o}(f) = \frac{A_V}{\beta^2}\left(\frac{f_{nc}}{|f|} + 1\right)\frac{f_V^2}{f^2 + f_V^2}, \tag{7}$$

where $f_V = \alpha_{ol}\beta/2\pi$ is the closed-loop bandwidth of the amplifier (in Hz) and $1/\beta$ is the DC gain. The power spectral density of the output voltage noise is plotted in Figure 4(b).

IV. CLOSED-LOOP POSITION NOISE

A. Noise sensitivity functions

To derive the closed-loop position noise, the response of the closed-loop system to each noise source must be considered. In particular, we need to specify the location where each source enters the feedback loop. The amplifier noise V_o appears at the plant input. In contrast, the external noise w acts at the plant output, and the sensor noise n_s disturbs the measurement.

A single axis feedback loop with additive noise sources is illustrated in Figure 5. For the sake of simplicity, the voltage amplifier is considered to be part of the controller. The transfer function from the amplifier voltage noise V_o to the position d is the input sensitivity function,

$$\frac{d(s)}{V_o(s)} = \frac{P(s)}{1 + C(s)P(s)}. \tag{8}$$

Likewise, the transfer function from the external noise w to the position d is the sensitivity function,

$$\frac{d(s)}{w(s)} = \frac{1}{1 + C(s)P(s)}. \tag{9}$$

Finally, the transfer function from the sensor noise n_s to the position d is the negated complementary sensitivity function,

$$\frac{d(s)}{n_s(s)} = \frac{-C(s)P(s)}{1 + C(s)P(s)} \tag{10}$$

B. Closed-loop position noise spectral density

With knowledge of the sensitivity functions and the noise power spectral densities, the power spectral density of the position noise due to each source can be derived. The position noise power spectral density due to the amplifier output voltage noise $S_{dV_o}(f)$ is

$$S_{dV_o}(f) = \frac{A_V}{\beta^2}\left(\frac{f_{nc}}{|f|} + 1\right)\frac{f_V^2}{f^2 + f_V^2}\left|\frac{d(j2\pi f)}{V_o(j2\pi f)}\right|^2. \tag{11}$$

Fig. 5. A single axis feedback control loop with a plant P and controller C.

Similarly, the position noise power spectral density due to the external force noise $S_{dw}(f)$ is

$$S_{dw}(f) = A_w \left| \frac{d(j2\pi f)}{w(j2\pi f)} \right|^2. \tag{12}$$

Finally, the position noise power spectral density due to the sensor noise $S_{dn_s}(f)$ is

$$S_{dn_s}(f) = A_s \cdot \left| \frac{d(j2\pi f)}{n_s(j2\pi f)} \right|^2. \tag{13}$$

The total position noise power spectral density $S_d(f)$ is the sum of the three individual sources,

$$S_d(f) = S_{dV_o}(f) + S_{dw}(f) + S_{dn_s}(f). \tag{14}$$

The position noise variance can also be found from the Wiener Khinchin relation

$$E\left[d^2\right] = \int_0^\infty S_d(f)\ df, \tag{15}$$

which is best evaluated numerically. If the noise is assumed to be Gaussian distributed, the 6σ-resolution of the nanopositioner is

$$6\sigma\text{-resolution} = 6\sqrt{E\left[d^2\right]} \tag{16}$$

C. Closed-loop noise approximations with integral control

If a simple integral controller is used, $C(s) = \alpha/s$, the transfer functions from the amplifier and external noise to displacement can be approximated by

$$\frac{d(s)}{V_o(s)} = \frac{sP(0)}{s + \alpha P(0)}, \qquad \frac{d(s)}{w(s)} = \frac{s}{s + \alpha P(0)}, \tag{17}$$

where $P(0)$ is the DC-Gain of the plant. Likewise, the complimentary sensitivity function can be approximated by

$$\frac{d(s)}{n_s(s)} = \frac{\alpha P(0)}{s + \alpha P(0)}. \tag{18}$$

With the above approximations of the sensitivity functions, the closed-loop position noise power spectral density can be derived. From (11) and (17) the position noise density due to the amplifier voltage noise $S_{dV_o}(f)$ is

$$S_{dV_o}(f) \approx \frac{A_V P(0)^2}{\beta^2} \left(\frac{f_{\text{nc}}}{|f|} + 1 \right) \frac{f_V^2}{f^2 + f_V^2} \frac{f^2}{f^2 + f_{cl}^2}, \tag{19}$$

where $f_{cl} = \frac{\alpha P(0)}{2\pi}$ is the closed-loop bandwidth. As illustrated in Figure 6(a), the position noise due to the amplifier has a bandpass characteristic with a mid-band density of $A_V P(0)^2/\beta^2$.

From (12) and (18) the position noise density due to the external noise $S_{dw}(f)$ is

$$S_{dw}(f) \approx A_w \frac{f^2}{f^2 + f_{cl}^2}, \tag{20}$$

which has a high-pass characteristic as illustrated in Figure 6(b) with a corner frequency equal to the closed-loop bandwidth.

The closed-loop position noise due to the sensor $S_{dn_s}(f)$ can be derived from (13) and (18), and is

$$S_{dn_s}(f) \approx A_s \frac{f_{cl}^2}{f^2 + f_{cl}^2}, \tag{21}$$

(a) The position noise power spectral density due to amplifier voltage noise $S_{dV_o}(f)$

(b) The position noise power spectral density due to external noise $S_{dw}(f)$

(c) The position noise power spectral density due to sensor noise $S_{dn_s}(f)$
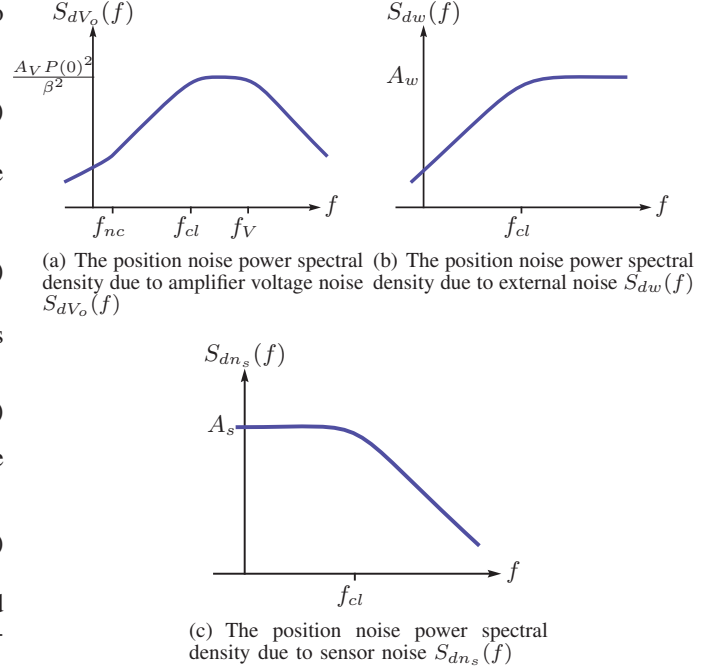
Fig. 6. The position noise power spectral density due to the amplifier voltage noise (a), external disturbance (b) and sensor noise (c).

which has a low-pass characteristic with a density of A_s and a corner frequency equal to the closed-loop bandwidth, as illustrated in Figure 6(c).

Although the expression for variance (15) is generally evaluated numerically, in some cases it is straightforward and useful to derive analytic expressions. One such case is the position noise variance due to sensor noise ($E\left[d^2\right]$ due to n_s) when integral control is applied. As demonstrated in the forthcoming examples, sensor noise is typically the dominant noise process in a feedback controlled nanopositioning system. As a result, other noise sources can sometimes by neglected.

As the sensor noise density is approximately constant and the sensitivity function (18) is approximately first-order, the resulting position noise can be determined from

$$\sqrt{E\left[d^2\right]} \text{ due to } n_s = \sqrt{A_s}\sqrt{1.57 f_{cl}}, \tag{22}$$

The corresponding 6σ-resolution is

$$6\sigma\text{-resolution} = 6\sqrt{A_s}\sqrt{1.57 f_{cl}}. \tag{23}$$

This expression can be used to determine the minimum resolution of a nanopositioning system given only the sensor noise density and closed-loop bandwidth. It can also be rearranged to reveal the maximum closed-loop bandwidth achievable given the sensor noise density and the required resolution.

$$\text{maximum bandwidth (Hz)} = \left(\frac{6\sigma\text{-resolution}}{7.51\sqrt{A_s}} \right)^2. \tag{24}$$

For example, consider a nanopositioner with integral feedback control and a capacitive sensor with a noise density of 30 pm$/\sqrt{\text{Hz}}$. The maximum bandwidth with a resolution of

Parameter	Value
Closed-loop bandwidth f_{cl}	50 Hz
Controller gain α	314
Amplifier bandwidth f_V	2 kHz
Amplifier gain $1/\beta$	50
Amplifier input voltage noise A_V	100 nV/$\sqrt{\text{Hz}}$
Amplifier output voltage noise	5 μV/$\sqrt{\text{Hz}}$
Amplifier noise corner frequency f_{nc}	100 Hz
Sensor noise A_s	20 pm/$\sqrt{\text{Hz}}$
Position range	100 μm
Sensitivity $P(0)$	500 nm/V
Resonance frequency ω_r	$2\pi \times 10^3$ r/s
Damping ratio ζ_r	0.05

TABLE I

SPECIFICATIONS OF AN EXAMPLE NANOPOSITIONING SYSTEM

(a) 50 Hz Closed-loop bandwidth

(b) 1 Hz Closed-loop bandwidth

Fig. 7. The spectral density of the total position noise $\sqrt{S_d(f)}$ and its two components, the amplifier output voltage noise $\sqrt{S_{dV_o}(f)}$ and sensor noise $\sqrt{S_{dn_s}(f)}$ (all in pm/$\sqrt{\text{Hz}}$).

1 nm is

$$\text{maximum bandwidth} = \left(\frac{1 \times 10^{-9}}{7.51 \times 30 \times 10^{-12}}\right)^2$$
$$= 11 \text{ Hz}$$

V. SIMULATION EXAMPLES

A. Integral controller noise simulation

In this section an example nanopositioner is considered with a range of 100 μm at 200 V and a resonance frequency of 1 kHz. The system model is

$$P(s) = 500 \frac{\text{nm}}{\text{V}} \times \frac{\omega_r^2}{s^2 + 2\omega_r\zeta_r s + \omega_r^2}, \qquad (25)$$

where $\omega_r = 2\pi 1000$ and $\zeta_r = 0.05$. The system includes a capacitive position sensor and voltage amplifier with the following specifications. The capacitive position sensor has a noise density of 20 pm/$\sqrt{\text{Hz}}$. The voltage amplifier has a gain of 20, a bandwidth of 2 kHz, an input voltage noise density of 100 nV/$\sqrt{\text{Hz}}$, and a noise corner frequency of 100 Hz.

The feedback controller in this example is a simple integral controller with compensation for the sensitivity of the plant, that is

$$C(s) = \frac{1}{500 \text{ nm/V}} \frac{\alpha}{s}, \qquad (26)$$

where α is the gain of the controller and also the approximate bandwidth (in rad/s) of the closed-loop system. All of the system parameters are summarized in Table I.

The total density of the position noise can now be calculated from equation (14). The total spectral density and its components are plotted in Figure 7(a). Clearly, the sensor noise is the dominant noise process. This is the case in most nanopositioning systems with closed-loop position feedback.
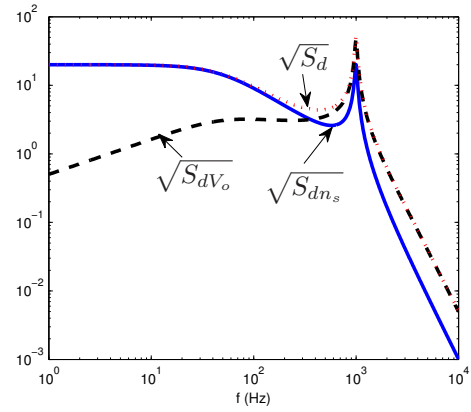
The variance of the position noise can be determined by solving the integral for variance numerically,

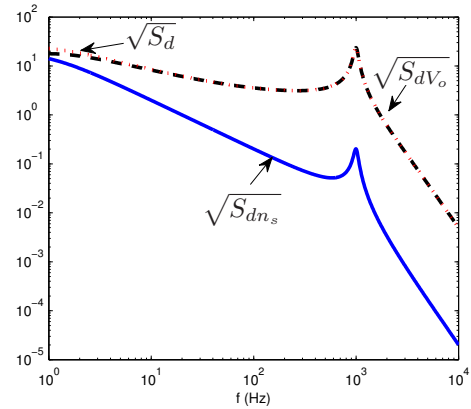$$\sigma^2 = E[d^2] = \int_0^\infty S_d(f) \, df \qquad (27)$$

The result is

$$\sigma^2 = 0.24 \text{ nm}^2, \text{ or } \sigma = 0.49 \text{ nm},$$

which implies a 6σ-resolution of 2.9 nm.

In systems with lower closed-loop bandwidth, the $1/f$ noise of the amplifier can become dominant. For example, if the closed-loop bandwidth of the previous example is reduced to 1 Hz, the new power spectral density, plotted Figure 7(b), differs significantly. The resulting variance and standard deviation are

$$\sigma^2 = 0.093 \text{ nm}^2, \text{ or } \sigma = 0.30 \text{ nm},$$

which implies a 6σ-resolution of 1.8 nm. Not a significant reduction considering that the closed-loop bandwidth has been reduced to 2% of its previous value. More generally, the resolution can be plotted against a range of closed-loop bandwidths to reveal the trend. In Figure 8, the 6σ-resolution is plotted against a range of closed-loop bandwidths from 100 mHz to 60 Hz. The curve has a minima of 1.8 nm at 0.4 Hz. Below this frequency, amplifier noise is the major contributor, while at higher frequencies, sensor noise is more significant.

B. Noise simulation with inverse model controller

In the previous example, the integral controller does not permit a closed-loop bandwidth greater than 100 Hz. Many other model-based controllers can achieve much better performance. One simple controller that demonstrates the noise characteristics of a model based controller is the combination of an integrator and notch filter, or direct inverse controller.
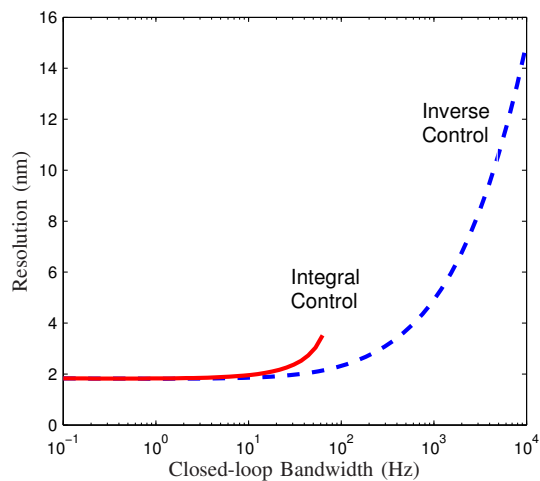
Fig. 8. Resolution of the example nanopositioning system with integral control (solid line) and inverse control (dashed).

The transfer function is an integrator combined with an inverse model of the plant,

$$C(s) = \frac{\alpha}{s} \frac{1}{500 \text{ nm/V}} \frac{s^2 + 2\omega_r \zeta_r s + \omega_r^2}{\omega_r}. \qquad (28)$$

The resulting loop-gain $C(s)P(s)$ is an integrator, so stability is guaranteed and the closed-loop bandwidth is α rad/s. With such a controller it is now possible to examine the noise performance of feedback systems with wide bandwidth.

Aside from improved bandwidth, the inverse controller also eliminates the resonance peak in the sensor induced noise spectrum. This benefit also occurs with controllers designed to damp the resonance peak [13]. After following the same procedure described in the previous section, the resulting variance for a closed-loop bandwidth of 500 Hz is

$$\sigma^2 = 0.37 \text{ nm}^2, \text{ or } \sigma = 0.61 \text{ nm},$$

which implies a 6σ-resolution of 3.7 nm. This is not significantly greater than the 50 Hz controller bandwidth in the previous example, which resulted in a 2.9 nm resolution. When the closed-loop bandwidth of the inverse controller is reduced to 50 Hz, the resolution is 2.1 nm, which is slightly better than the previous example. The difference is due to the absence of the resonance peak in the sensor induced noise.

The resolution of the inverse controller is plotted for a wide range of bandwidths in Figure 8. The minimum resolution is 1.8 nm at 1 Hz. After approximately 100 Hz, the position noise is due predominantly to the sensor-noise which is proportional to the square-root of closed-loop bandwidth, as described in equation (23).

C. Feedback versus feedforward control

A commonly discussed advantage of feedforward control systems is the absence of sensor induced noise. However, this view does not take into account the presence of $1/f$ amplifier noise that can result in significant peak-to-peak amplitude.

It is not necessary to derive equations for the noise performance of feedforward systems as this is a special case of the feedback examples already discussed. The positioning noise of a feedforward control system is equivalent to a feedback control system when $C(s) = 0$ or equivalently,

when the closed-loop bandwidth is zero. Thus, the plots of resolution versus bandwidth in Figure 8 are also valid for feedforward control. The feedforward controller resolution is the DC resolution of these plots, which in both cases is 2.60 nm.

It is interesting to note that both the integral and inverse controller can achieve slightly less positioning noise than a feedforward control system when the closed-loop bandwidth is very low. This is because the amplifier noise density is greater than the sensor noise density at low frequencies. In the examples considered, the optimal noise performance could be achieved with a feedback controller of around 1-Hz bandwidth. To increase the positioning bandwidth, a feedforward input would be required [14].

VI. CONCLUSIONS

In this article, a frequency domain approach was used to quantify noise sources and predict the closed-loop resolution of a nanopositioning system. The foremost noise sources were identified as the amplifier voltage noise and the displacement sensor noise. Simulation examples demonstrate that the minimum positioning noise usually occurs in open-loop or with very low closed-loop bandwidth. This implies that combined feedback and feedforward control can achieve the best positioning resolution.

REFERENCES

[1] S. Devasia, E. Eleftheriou, and S. O. R. Moheimani, "A survey of control issues in nanopositioning," *IEEE Transactions on Control Systems Technology*, vol. 15, no. 5, pp. 802–823, September 2007.
[2] S. M. Salapaka and M. V. Salapaka, "Scanning probe microscopy," *IEEE Control Systems Magazine*, vol. 28, no. 2, pp. 65–83, April 2008.
[3] S. Mishra, J. Coaplen, and M. Tomizuka, "Precision positioning of wafer scanners. segmented iterative learning control for nonrepetitive disturbances," *IEEE Control Systems*, vol. 27, no. 4, pp. 20–25, August 2007.
[4] A. Sebastian, A. Pantazi, H. Pozidis, and E. Elefthriou, "Nanopositioning for probe-based data storage," *IEEE Control Systems*, vol. 28, no. 4, pp. 26–35, August 2008.
[5] A. J. Fleming, "Nanopositioning system with force feedback for high-performance tracking and vibration control," *IEEE Transactions on Mechatronics*, vol. 15, no. 3, pp. 433–447, June 2010.
[6] A. Al Mamun and S. S. Ge, "Precision control of hard disk drives," *Control Systems, IEEE*, vol. 25, no. 4, pp. 14 – 19, aug. 2005.
[7] D. Abramovitch and G. Franklin, "A brief history of disk drive control," *Control Systems, IEEE*, vol. 22, no. 3, pp. 28 –42, jun 2002.
[8] "ISO 5725 - accuracy (trueness and precision) of measurement methods and results, interational organization for standardization," 1994.
[9] D. S. Nyce, *Linear position sensors. Theory and application.* John Wiley and Sons, 2004.
[10] J. Fraden, *Handboook of modern sensors: physics, designs, and applications.* New York: Springer, 2004.
[11] W. C. van Etten, *Introduction to noise and random processes.* West Sussex, England: John Wiley and Sons, 2005.
[12] R. G. Brown and P. Y. C. Hwang, *Introduction to random signals and applied kalman filtering.* John Wiley and Sons, 1997.
[13] A. J. Fleming, S. S. Aphale, and S. O. R. Moheimani, "A new method for robust damping and tracking control of scanning probe microscope positioning stages," *IEEE Transactions on Nanotechnology*, vol. 9, no. 4, pp. 438–448, September 2010.
[14] K. K. Leang, Q. Zou, and S. Devasia, "Feedforward control of piezoactuators in atomic force microscope systems," *IEEE Control Systems*, vol. 29, no. 1, pp. 70–82, February 2009.